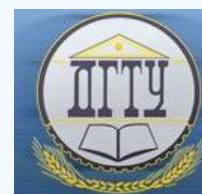


MECHANICS



UDC 624.04

<https://doi.org/10.23947/2687-1653-2021-21-2-114-122>

Stability analysis of wooden arches with account for nonlinear creep



S. B. Yazyev¹, V. I. Andreev², A. S. Chepurnenko¹

¹ Don State Technical University (Rostov-on-Don, Russian Federation)

² Moscow State University of Civil Engineering (Moscow, Russian Federation)

Introduction. The paper deals with the calculation of wooden arches taking into account the nonlinear relationship between stresses and instantaneous deformations, as well as creep and geometric nonlinearity, are considered. The analysis is based on the integral equation of the viscoelastoplastic hereditary aging model, originally proposed by A.G. Tamrazyan [1] to describe the nonlinear creep of concrete.

Materials and Methods. The creep measure is taken in accordance with the work of I.E. Prokopovich and V.A. Zedgenidze [2] as a sum of exponential functions. The transition from the integral form of the creep law to the differential form is shown. The relationship between stresses and instantaneous deformations for wood under compression is determined from the Gerstner formula, and elastic work is assumed under tension. The solution is carried out using the finite element method in combination with the Newton-Raphson method and the Euler method according to the scheme that involves a stepwise increase in the load with correction of the stiffness matrix taking into account the change in the coordinates of the nodes with the sequential calculation of additional displacements of the nodes, which are due to the residual forces. The proposed approach for increasing the accuracy of determination of creep deformations at each step provides using the fourth-order Runge-Kutta method instead of the Euler method.

Results. Based on the Lagrange variational principle, expressions are obtained for the stiffness matrix and the vector of additional dummy loads due to creep. The method developed by the authors is implemented in the form of a program in the MATLAB environment. Calculation examples are given for parabolic arches simply supported at the ends without an intermediate hinge and with an intermediate hinge in the middle of the span under the action of a uniformly distributed load. The results obtained are compared in the viscoelastic and viscoelastic formulation. The reliability of the results is validated through the calculation in the elastic formulation in the ANSYS software package.

Discussion and Conclusions. For the arches considered, it is found that even with a load close to the instant critical, the growth of time travel is limited. Thus, the nature of their work under creep conditions differs drastically from the nature of the deformation of compressed rods.

Keywords: creep, wooden arch, geometric nonlinearity, viscoelastic plasticity, finite element method.

For citation: S. B. Yazyev, V. I. Andreev, A. S. Chepurnenko. Stability analysis of wooden arches with account for nonlinear creep. Advanced Engineering Research, 2021, vol. 21, no. 2, pp. 114–122. <https://doi.org/10.23947/2687-1653-2021-21-2-114-122>

© Yazyev S. B., Andreev V. I., Chepurnenko A. S., 2021



Introduction. Wood refers to the materials that exhibit their non-linear properties, both under short-term and long-term exposure. Most existing rheological models of wood establish its instantaneous properties on the basis of Hooke's law; but for compressed wood, a nonlinear diagram of the elastoplastic type is typical [3]. K. P. Pyatikrestovskiy was the first to investigate the issues of joint accounting of instantaneous elastoplastic properties of wood and its creep. He combined these properties on the basis of the method of modulus of long-term deformation [4–7]. In this method, the creep equation contains time explicitly, which significantly limits its use in the case of

complex loading modes and variable loads. There is a significant number of publications on the joint accounting of creep and instantaneous nonlinearity of wood deformation in the calculation of compressed rods [8–14]. In particular, [8] discusses the applicability of the Boltzmann superposition principle to the description of nonlinear wood creep. In [9], theoretical calculations are compared to experimental data for compressed rods; and in [10], in addition to the compressive longitudinal load, the transverse load is taken into account. In [11–13], the stability problem is solved for the rod elements in the frame structure. In paper [14], a long-term critical force is derived for compressed wooden elements, taking into account the nonlinear creep.

The problem of calculation with account for creep and instantaneous nonlinearity of deformation is a challenge not only for any particular rod and frame, but also for such rod systems as arches. This work objective is to develop a method for calculating arch structures taking into account the nonlinear properties of the material under short-term and long-term exposure, as well as geometric nonlinearity.

Materials and Methods. As a relation that determines the relationship between stresses and deformations, we use the equation of the viscoelastic model of hereditary aging:

$$\varepsilon(t) = \frac{f[\sigma(t)]}{E_0(t)} - \int_{\tau_0}^t [f[\sigma(\tau)]] \frac{\partial C(t, \tau)}{\partial \tau} d\tau, \quad (1)$$

This equation was first proposed in [1] for modeling the nonlinear creep of concrete. Here, the function $f(\sigma)$ establishes the relationship between stress and instantaneous strain, $C(t, \tau)$ — creep measure. The stress-strain diagram of compressed wood under short-term loading is well approximated by the Gerstner formula [15], which has the form:

$$\sigma = E_0 \varepsilon - \frac{E_0^2}{4R} \varepsilon^2. \quad (2)$$

The compressive stresses are used in the formula (2) with the sign “+”. When wood is stretched, there is a linear diagram up to the breaking point. Expressing the strain in terms of stress from (2), we obtain:

$$\varepsilon = \frac{2R}{E_0} \left(1 - \sqrt{1 - \frac{\sigma}{R}} \right). \quad (3)$$

Based on (3), the stress function $f(\sigma)$ can be written as:

$$f(\sigma) = 2R \left(1 - \sqrt{1 - \frac{\sigma}{R}} \right). \quad (4)$$

To measure the creep of wood, we use the formula proposed in the work of V. A. Zedgenidze and I. E. Prokopovich [2]:

$$C(t, \tau) = (C_0 + A_0 e^{-\gamma \tau}) [1 - B_1 e^{-\gamma(t-\tau)}], \quad (5)$$

where $C_0 = 2.87 \cdot 10^{-5} \text{ MPa}^{-1}$, $A_0 = 10.95 \cdot 10^{-5} \text{ MPa}^{-1}$, $B_1 = 1$, $\gamma = \gamma_1 = 0.15 \text{ day}^{-1}$.

Equation (1) can be presented in the form:

$$\varepsilon = \frac{\sigma}{E} + \varepsilon^*, \quad (6)$$

where $E = \frac{E_0 \sigma}{f(\sigma)}$ — secant modulus, $\varepsilon^* = - \int_{\tau_0}^t [f[\sigma(\tau)]] \frac{\partial C(t, \tau)}{\partial \tau} d\tau$ — creep deformation.

For the creep measure in the form (5), the creep strain can be written as the sum of two components:

$$\varepsilon^* = \varepsilon_1^* + \varepsilon_2^*, \quad \varepsilon_1^* = \gamma C_0 B_1 \int_{\tau_0}^t [f[\sigma(\tau)]] e^{-\gamma(t-\tau)} d\tau, \quad \varepsilon_2^* = A_0 \gamma \int_{\tau_0}^t [f[\sigma(\tau)]] e^{-\gamma \tau} d\tau. \quad (7)$$

Differentiating in time (7), we obtain expressions for the growth rates of each component:

$$\frac{\partial \varepsilon_1^*}{\partial t} = \gamma (C_0 B_1 f[\sigma(t)] - \varepsilon_1^*); \quad \frac{\partial \varepsilon_2^*}{\partial t} = A_0 \gamma f[\sigma(t)] e^{-\gamma t}. \quad (8)$$

On the basis of (6), we derive the relationship between internal forces and deformations for the element under the combined action of the longitudinal force and the bending moment. The elastic modulus is assumed to be a function of y coordinate, which varies from $-h/2$ to $h/2$ in the height of the cross section. Based on the hypothesis of flat sections, we write the total deformation in the form:

$$\varepsilon = \varepsilon_0 + y\chi, \tag{9}$$

where ε_0 — deformation of the middle layer $\chi = -\frac{d^2v}{dx^2}$ — change in curvature..

We then substitute (9) in (6). Expressing σ by ε , we obtain:

$$\sigma = E(y)(\varepsilon - \varepsilon^*) = E(y)(\varepsilon_0 + y\chi - \varepsilon^*). \tag{10}$$

The longitudinal force and bending moment in the element are related to the stress through the following integral dependences:

$$M = \int_A \sigma y dA; \quad N = \int_A \sigma dA. \tag{11}$$

Here, A — cross-sectional area of the rod.

Substitute (10) in (11) and convert the resulting equalities to the matrix form:

$$\begin{Bmatrix} N \\ M \end{Bmatrix} = [D] \begin{Bmatrix} \varepsilon_0 \\ \chi \end{Bmatrix} - \begin{Bmatrix} N^* \\ M^* \end{Bmatrix}, \tag{12}$$

where $N^* = \int_A E(y)\varepsilon^* dA$, $M^* = \int_A E(y)y\varepsilon^* dA$, $[D] = \begin{bmatrix} EA & ES \\ ES & EI \end{bmatrix}$ — the matrix of reduced stiffnesses, which are determined from the formulas:

$$EA = \int_A E(y) dA, \quad ES = \int_A E(y) y dA, \quad EI = \int_A E(y) y^2 dA. \tag{13}$$

The problem with account for the physical and geometric nonlinearity will be solved by the authors using the finite element method. The rod element shown in Fig. 1 is used. The axial strain, taking into account the geometric nonlinearity, is the sum of the linear and nonlinear components:

$$\varepsilon_0 = \varepsilon_0' + \varepsilon_0'' = \frac{du}{dx} + \frac{1}{2} \left(\frac{dv}{dx} \right)^2. \tag{14}$$

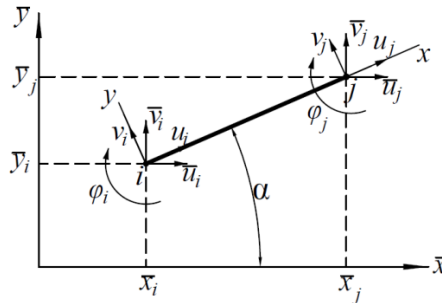


Fig. 1. Rod finite element

To obtain a system of FEM equations, we use the Lagrange variational principle. The strain potential energy (SPE) is written as:

$$\Pi = \frac{1}{2} \int_V \sigma \varepsilon^{el} dV = \frac{1}{2} \int_V E(y) (\varepsilon_0' + \varepsilon_0'' + y\chi - \varepsilon^*)^2 dV. \tag{15}$$

where ε^{el} — elastic strain, equal to the difference between total strain and creep strain.

We write (15) as the sum of four integrals:

$$\begin{aligned} \Pi = \frac{1}{2} & \left(\int_V E(y) \varepsilon_0' (\varepsilon_0' + \varepsilon_0'' + y\chi - \varepsilon^*) dV + \int_V E(y) \varepsilon_0'' (\varepsilon_0' + \varepsilon_0'' + y\chi - \varepsilon^*) dV + \right. \\ & \left. + \int_V E(y) y\chi (\varepsilon_0' + \varepsilon_0'' + y\chi - \varepsilon^*) dV - \int_V E(y) \varepsilon^* (\varepsilon_0' + \varepsilon_0'' + y\chi - \varepsilon^*) dV \right) \end{aligned} \tag{16}$$

The first integral in (16) is written as:

$$\int_V E(y) \varepsilon_0' (\varepsilon_0' + \varepsilon_0'' + y\chi - \varepsilon^*) dV = \int_0^l \varepsilon_0' \int_A E(y) (\varepsilon_0' + y\chi - \varepsilon^*) dA dx + \tag{17}$$

$$+\int_0^l \varepsilon_0' \cdot \varepsilon_0^n \int_A E(y) dAdx = \int_0^l \varepsilon_0' N dx + \int_0^l \varepsilon_0' \cdot \varepsilon_0^n \cdot EAdx,$$

where l — the length of the finite element.

The second integral in (16) is presented in the following form:

$$\begin{aligned} \int_V E(y) \varepsilon_0^n (\varepsilon_0' + \varepsilon_0^n + y\chi - \varepsilon^*) dV &= \int_0^l \varepsilon_0' \cdot \varepsilon_0^n \int_A E(y) dAdx + \int_V E(y) (\varepsilon_0^n)^2 dV + \\ &+ \int_0^l \varepsilon_0^n \cdot \chi \int_A E(y) y dAdx - \int_0^l \varepsilon_0^n \int_A E(y) \varepsilon^* dAdx, \end{aligned} \quad (18)$$

The second term in the right-hand side of (18) can be neglected, given its higher order of smallness. The third integral in (16) is written as:

$$\begin{aligned} \int_V E(y) y \chi (\varepsilon_0' + \varepsilon_0^n + y\chi - \varepsilon^*) dV &= \int_0^l \chi \int_A E(y) y (\varepsilon_0' + y\chi - \varepsilon^*) dAdx + \\ &+ \int_0^l \varepsilon_0' \chi \cdot ESdx = \int_0^l M \chi dx + \int_0^l \varepsilon_0^n \chi \cdot ESdx. \end{aligned} \quad (19)$$

The fourth integral in (16) is presented in the following form:

$$\begin{aligned} \int_V E(y) \varepsilon^* (\varepsilon_0' + \varepsilon_0^n + y\chi - \varepsilon^*) dV &= \int_0^l \chi \int_A E(y) y \varepsilon^* dAdx + \\ &+ \int_0^l \varepsilon_0' \int_A \varepsilon^* E(y) dAdx - \int_V (\varepsilon^*)^2 E(y) dV + \int_0^l \varepsilon_0^n \int_A \varepsilon^* E(y) dAdx = \\ &= \int_0^l \chi M^* dx + \int_0^l \varepsilon_0' N^* dx + \int_0^l \varepsilon_0^n N^* dx - \int_V (\varepsilon^*)^2 E(y) dV. \end{aligned} \quad (20)$$

The summand $\int_V (\varepsilon^*)^2 E(y) dV$ when minimized over the vector of nodal displacements, will vanish. Finally, the expression for the SPE will take the form:

$$\begin{aligned} \Pi &= \frac{1}{2} \left(\int_0^l \varepsilon_0' N dx + 2 \int_0^l \varepsilon_0' \varepsilon_0^n EA dx + \int_0^l M \chi dx + 2 \int_0^l \varepsilon_0^n \chi ES dx - \int_0^l \chi M^* dx - \int_0^l \varepsilon_0' N^* dx + \right. \\ &\left. + 2 \int_0^l \varepsilon_0^n N^* dx \right) = \frac{1}{2} \int_0^l \left\{ \varepsilon_0' \quad \chi \right\} \left(\begin{Bmatrix} N \\ M \end{Bmatrix} - \begin{Bmatrix} N^* \\ M^* \end{Bmatrix} \right) dx + N_{av} \int_0^l \varepsilon_0^n dx, \end{aligned} \quad (21)$$

where $N_{av} = \varepsilon_0' EA + \chi_{av} ES - N^*$ — the average axial force in the element, χ_{av} — the mean change in the curvature of the element.

Taking into account (12), formula (21) will take the form:

$$\Pi = \frac{1}{2} \int_0^l \left\{ \varepsilon \right\}^T \left([D] \left\{ \varepsilon \right\} - 2 \begin{Bmatrix} N^* \\ M^* \end{Bmatrix} \right) dx + N_{av} \int_0^l \varepsilon_0^n dx, \quad (22)$$

where $\left\{ \varepsilon \right\}^T = \left\{ \varepsilon_0' \quad \chi \right\}^T$.

For finite element displacements, we assume the following approximation:

$$u(x) = u_1 + \frac{u_2 - u_1}{l} x; \quad (23)$$

$$v(x) = \alpha_1 + \alpha_2 x + \alpha_3 x^2 + \alpha_4 x^3; \quad (24)$$

$$\varphi(x) = \frac{dv}{dx} = \alpha_2 + 2\alpha_3 x + 3\alpha_4 x^2. \quad (25)$$

The coefficients of polynomial (24) are determined through substituting the coordinates of the following nodes in (24) and (25):

$$\begin{bmatrix} 1 & 0 & 0 & 0 \\ 0 & 1 & 0 & 0 \\ 1 & l & l^2 & l^3 \\ 0 & 1 & 2l & 3l^2 \end{bmatrix} \cdot \begin{pmatrix} \alpha_1 \\ \alpha_2 \\ \alpha_3 \\ \alpha_4 \end{pmatrix} = \begin{pmatrix} v_1 \\ \varphi_1 \\ v_2 \\ \varphi_2 \end{pmatrix}. \quad (26)$$

From (26), vector $\{\alpha\} = \{\alpha_1 \ \alpha_2 \ \alpha_3 \ \alpha_4\}^T$ is expressed as follows:

$$\{\alpha\} = \begin{bmatrix} 1 & 0 & 0 & 0 \\ 0 & 1 & 0 & 0 \\ 1 & l & l^2 & l^3 \\ 0 & 1 & 2l & 3l^2 \end{bmatrix}^{-1} \cdot \begin{pmatrix} v_1 \\ \varphi_1 \\ v_2 \\ \varphi_2 \end{pmatrix} = \begin{bmatrix} 0 & 1 & 0 & 0 & 0 & 0 \\ 0 & 0 & 1 & 0 & 0 & 0 \\ 0 & -\frac{3}{l^2} & -\frac{2}{l} & 0 & \frac{3}{l^2} & -\frac{1}{l} \\ 0 & \frac{2}{l^3} & \frac{1}{l^2} & 0 & -\frac{2}{l^3} & \frac{1}{l^2} \end{bmatrix} \cdot \begin{pmatrix} u_1 \\ v_1 \\ \varphi_1 \\ u_2 \\ v_2 \\ \varphi_2 \end{pmatrix} = [\Phi]\{U\}. \quad (27)$$

Taking into account (27), formula (24) will take the form:

$$v = \{\Psi\}\{U\}, \quad (28)$$

$$\text{где } \Psi = \{1 \ x \ x^2 \ x^3\}[\Phi].$$

Vector $\{\varepsilon\}$ is written as:

$$\{\varepsilon\} = \begin{pmatrix} \frac{du}{dx} \\ -\frac{d^2v}{dx^2} \end{pmatrix} = \begin{bmatrix} -1/l & 0 & 0 & 1/l & 0 & 0 \\ -\frac{d^2\{\Psi\}}{dx^2} \end{bmatrix} \cdot \{U\} = [B]\{U\}. \quad (29)$$

After substituting (29) and (28) in (22), the SPE is written as:

$$\Pi = \frac{1}{2} \{U\}^T \int_0^l [B]^T [D] [B] dx \{U\} - \{U\}^T \int_0^l [B]^T dx \begin{Bmatrix} N^* \\ M^* \end{Bmatrix} + \{U\}^T N_{av} \cdot \frac{1}{2} \int_0^l \frac{d\{\Psi\}^T}{dx} \frac{d\{\Psi\}}{dx} dx \{U\}. \quad (30)$$

After minimizing the Lagrange functional with respect to the nodal displacement vector, we arrive at a system of equations of the following form:

$$([K] + [K_g])\{U\} = \{F\} + \{F^*\}, \quad (31)$$

where $[K] = \int_0^l [B]^T [D] [B] dx$ — stiffness matrix, $[K_g] = N_{av} \int_0^l \frac{d\{\Psi\}^T}{dx} \frac{d\{\Psi\}}{dx} dx$ — geometric stiffness matrix,

$\{F^*\} = \int_0^l [B]^T dx \begin{Bmatrix} N^* \\ M^* \end{Bmatrix}$ — contribution to the load vector of creep strains, $\{F\}$ — vector of external nodal forces.

A physically and geometrically nonlinear problem is solved using the Newton-Raphson method. The first step is the calculation at $t = 0$. The load increment is performed in quasi-statically small portions with the sequential calculation of additional displacements of the nodes, which are caused by the residual forces, the adjustment of the tangent modulus of elasticity and the coordinates of the nodes at each step.

Next, the time interval at which the calculation is performed is divided into a finite number of time steps. The creep calculation is performed in the same way as the static load calculation. The increment of creep deformations at the step $t+\Delta t$ can be determined using the Euler method

$$\Delta \varepsilon^* = \left(\frac{\partial \varepsilon_1^*}{\partial t} + \frac{\partial \varepsilon_2^*}{\partial t} \right) \Delta t. \quad (32)$$

Research Results. The presented equations and the calculation algorithm are implemented by the authors in the form of a program in the MATLAB environment. The calculation of a parabolic arch simply supported at the ends under the action of a load evenly distributed along the length was performed (Fig. 2) with the following initial data: $E_0 = 1.48 \cdot 10^4$ MPa, $R = 55$ MPa, $L = 16$ m, $f = 3.2$ m. The cross-section of the arch was assumed to be rectangular with dimensions $b = 10$ cm, $h = 15$ cm. The arch was divided into 40 finite elements in length, the section was divided into

100 segments in height, the number of steps in time was assumed to be 600, and in load — 200. The maximum number of iterations at each step is 20. Figure 3 shows the maximum deflection versus load graph. The dashed line corresponds to the calculation in the elastic formulation. To check the results, the solution to the elastic problem was also performed in the ANSYS software package using BEAM 188 rod finite elements. The number of finite elements was assumed to be the same as in MATLAB. There was no significant difference in the results. When calculating in the elastic formulation, a sharp increase in displacements corresponding to the loss of stability is observed at $q = 10.5$ kN/m, and when taking into account the instantaneous nonlinearity of deformation — at $q = 10$ kN/m.

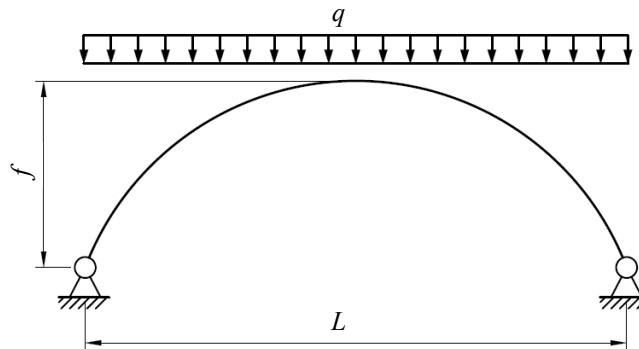


Fig. 2. Design scheme of the structure

q — distributed load on the arch, f — arch rise, L — arch span

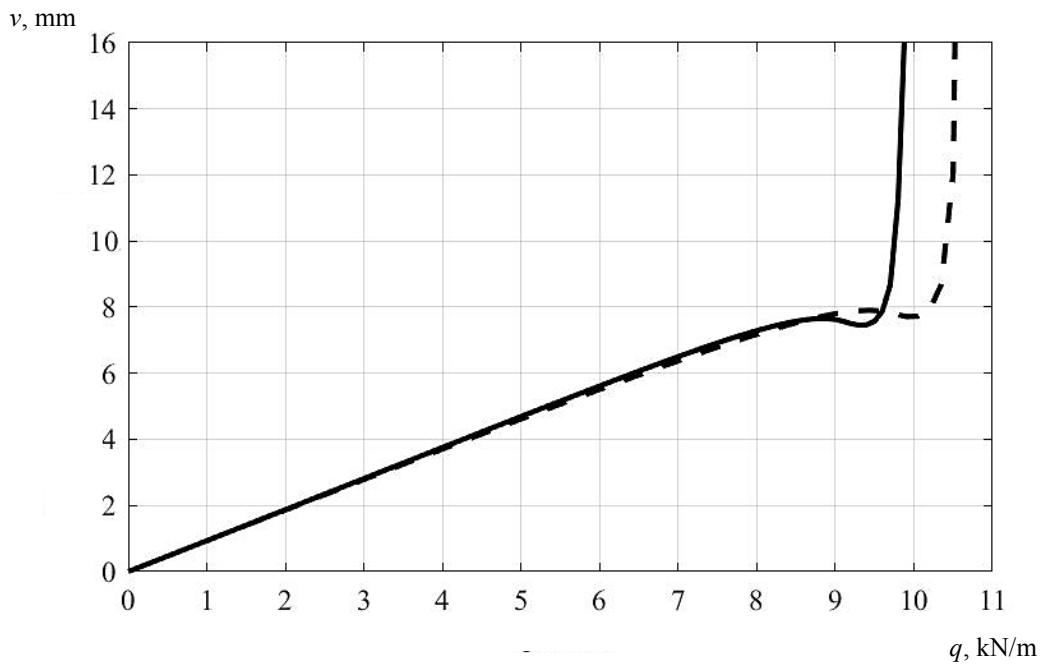


Fig. 3. Dependence of maximum arch deflection on the load under short-term loading

The creep calculation for this arch has shown that even at loads close enough to the instantaneous critical load, the growth of displacements is limited. Figure 4 shows a graph of the midspan deflection growth versus time under a load of $q = 8$ kN/m. The dashed line on this graph corresponds to the solution in the viscoelastic formulation. There was no significant difference in the results.

Also, with the above initial data, the calculation of a three-pinned arch with an intermediate hinge in the middle of the span was performed. In this case, the instantaneous critical load was significantly lower. When calculated in the elastic formulation, it was 4 kN/m, and with account for the instantaneous nonlinearity of deformation — 3.3 kN/m. As in the previous example, even when the load is close enough to the instantaneous critical, the creep decays. The curves of change in time of maximum deflection at $q = 3$ kN/m are shown in Fig. 5. The symbols are the same as in the previous graph.

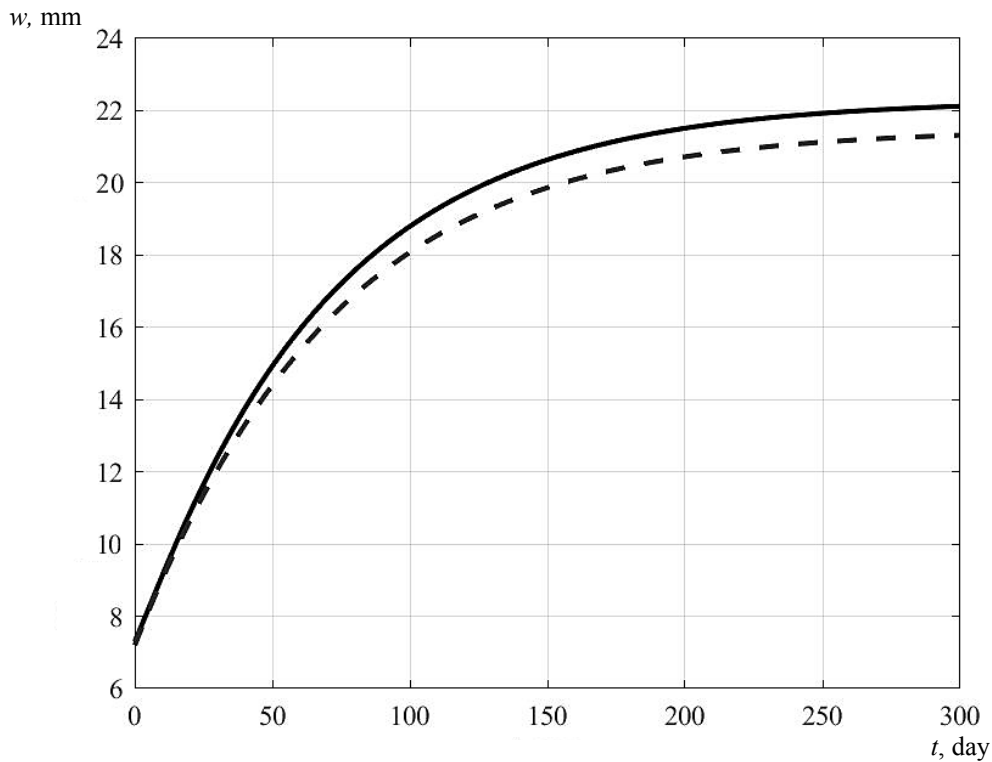


Fig. 4. Change in deflection in the middle of the span over time under load $q = 8 \text{ kN/m}$

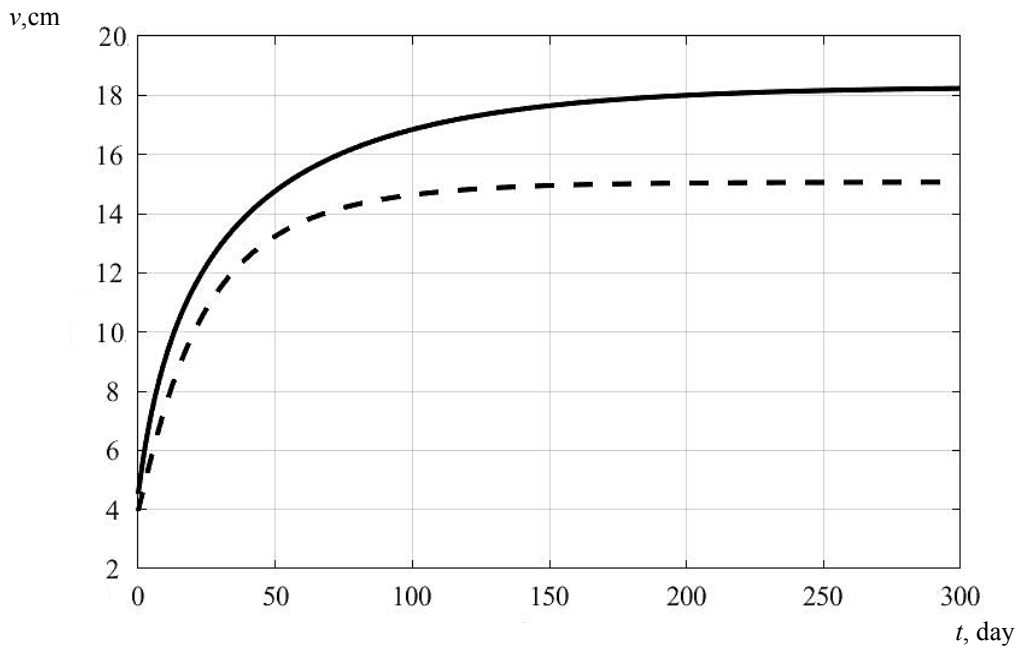


Fig. 5. The growth in time of maximum deflection for an arch with an intermediate hinge in the middle of the span at $q = 3 \text{ kN/m}$

Discussion and Conclusions. The resulting equations and the developed method are universal and provide the use of arbitrary dependences between stresses and instantaneous strains, as well as arbitrary expressions for the creep measure. This provides calculations of structures made not only of wood, but also of any other material. As a result of the analysis of the creep of wooden arches, it is found that, in contrast to compressed rods, creep is limited for them, even under loads close to the instantaneous critical load.

References

1. Tamrazyan AG, Esayan SG. Mekhanika polzuchesti betona [Mechanics of concrete creep]. Moscow: MGSU; 2011. 320 p. (In Russ.)
2. Prokopovich IE, Zedgenidze VA. Prikladnaya teoriya polzuchesti [Applied creep theory]. Moscow: Stroiizdat; 1980. 239 p. (In Russ.)

3. Varenik AS, Varenik KA. O polzuchesti drevesiny [Regarding creep of wood]. Modern Problems of Science and Education. 2014;2:88. URL: <http://www.science-education.ru/pdf/2014/2/429.pdf> (accessed: 19.03.2021). (In Russ.)
4. Pyatikrestovskiy KP, Travush VI. O programmirovanii nelineinogo metoda rascheta derevyannykh konstruktssii [Nonlinear method programming for calculations of statistically indeterminate wooden structures and software systems' communication to development of improved design standards]. Academia. Architecture and Construction. 2015;2:115–119. (In Russ.)
5. Pyatikrestovskiy KP, Sokolov BS. Nonlinear analysis of statically indeterminate wooden structures and optimization of cross section dimensions of dome ribs. International Journal for Computational Civil and Structural Engineering. 2018;14(4):130–139.
6. Pyatikrestovskiy KP, Travush VI, Pogoreltsev AA, et al. Development of structures from solid wood for objects of infrastructure. International Journal for Computational Civil and Structural Engineering. 2018;14(1):145–154. <https://doi.org/10.22337/2587-9618-2018-14-1-145-154>
7. Pyatikrestovskiy KP, Sokolov BS. The Study of Complex Stress States of Elements Filling the Cells Between the Ribs of Wooden Large-Span Domes. International Journal for Computational Civil and Structural Engineering. 2019;15(1):140–152.
8. Varenik KA, Varenik AS, Sanzharovskiy RS. Boltzmann principle of superposition in the theory of wood creep for deformations in time. IOP Conference Series: Materials Science and Engineering. 2018;441(1):012057. URL: <https://iopscience.iop.org/article/10.1088/1757-899X/441/1/012057/meta>
9. Varenik KA, Varenik AS, Kirillov AV, et al. Short-term and long-term longitudinal load tests of wooden rods. IOP Conference Series: Materials Science and Engineering. 2020;939(1):012080. URL: <https://iopscience.iop.org/article/10.1088/1757-899X/939/1/012080/meta>
10. Varenik AS, Varenik KA. Model of stress-strain state of wooden rod under eccentric compression and transverse load. IOP Conference Series: Materials Science and Engineering. 2019;656(1):012052. URL: <https://iopscience.iop.org/article/10.1088/1757-899X/656/1/012052/pdf>
11. Dubrakova KO, Dubrakov SV, Altuhov FV, et al. The buckling of the physically nonlinear frame-rod structural systems. IOP Conference Series: Materials Science and Engineering. 2019;698(2):022007. <https://doi.org/10.1088/1757-899X/698/2/022007>
12. Dmitrieva KO. Voprosy ustoychivosti sterzhnevyykh ehlementov konstruktivnykh sistem iz drevesiny pri silovom i sredovom nagruzhenii [Issues of stability of core elements of structural systems made of wood under force and environmental loading]. Building and Reconstruction. 2016;4:13–18. (In Russ.)
13. Klyuyeva NV, Dmitrieva KO. Voprosy ustoychivosti sterzhnevyykh ehlementov konstruktivnykh sistem iz drevesiny razlichnykh porod pri silovom i sredovom nagruzhenii v usloviyakh povyshennoi vlazhnosti [Issues of sustainable rod elements design systems of different wood species in force and environmental loading moisture]. Building and Reconstruction. 2016;5:60–68. (In Russ.)
14. Varenik AS, Varenik KA. Dlitel'naya nesushchaya sposobnost' derevyannykh konstruktssii [Long bearing capacity of wooden structure]. Structural Mechanics of Engineering Constructions and Buildings. 2014;2:23–30. (In Russ.)
15. Pyatikrestovskiy KP. K voprosu o vybore modulei uprugosti pri raschete derevyannykh konstruktssii na prochnost', ustoychivost' i po deformatsiyam [On the selection of elastic moduli in the calculation of wooden structures for strength, stability and deformations]. Structural Mechanics and Analysis of Constructions. 2012;6:73–79. (In Russ.)

Received 28.04.2021

Revised 30.05.2021

Accepted 31.05.2021

About the Authors:

Yazyev, Serdar B., associate professor of the Engineering Mechanics Department, Don State Technical University (1, Gagarin sq., Rostov-on-Don, RF, 344003), Cand.Sci. (Eng.), associate professor, ScopusID: [57190970024](https://orcid.org/57190970024), ORCID: <http://orcid.org/0000-0002-7839-7381>, russiangel@mail.ru

Andreev, Vladimir I., Head of the Strength of Materials Department, Moscow State University of Civil Engineering (26, Yaroslavskoye Shosse, Moscow, RF, 129337), Dr.Sci. (Eng.), professor, member of Russian Academy of

Architecture and Construction Sciences, ResearcherID: [T-9006-2017](https://orcid.org/0000-0002-1057-4329), ScopusID: [57198780961](https://orcid.org/0000-0002-1057-4329), ORCID: <https://orcid.org/0000-0002-1057-4329>, asv@mgsu.ru

Chepurnenko, Anton S., associate professor of the Strength of Materials Department, Don State Technical University (1, Gagarin sq., Rostov-on-Don, RF, 344003), Cand.Sci. (Eng.), ResearcherID: [E-4692-2017](https://orcid.org/0000-0002-9133-8546), ScopusID: [56056531000](https://orcid.org/0000-0002-9133-8546), ORCID: <https://orcid.org/0000-0002-9133-8546>, anton_chepurnenk@mail.ru

Claimed contributorship

S. B. Yazyev: basic concept formulation; obtaining resolving equations; computational analysis; text preparation; formulation of conclusions. V. I. Andreev: academic advising; analysis of the research results; the text revision; correction of the conclusions. A. S. Chepurenko: participation in the development of the calculation program; analysis of the research results; the text revision; correction of the conclusions.

All authors have read and approved the final manuscript.